

Refined critical balance in strong Alfvénic turbulence

A. Mallet,^{1,2,3} A. A. Schekochihin,^{1,4} and B. D. G. Chandran,^{3,4}

¹Rudolf Peierls Centre for Theoretical Physics, University of Oxford, 1 Keble Rd, Oxford OX1 3NP, UK

²Wolfgang Pauli Institute, Faculty of Mathematics, University of Vienna, Oskar-Morgenstern-Platz 1, 1090 Vienna, Austria

³Space Science Center and Department of Physics, University of New Hampshire, Durham, NH 03824, USA

⁴Merton College, Oxford OX1 4JD, UK

18 October 2018

ABSTRACT

We present numerical evidence that in strong Alfvénic turbulence, the critical balance principle—equality of the nonlinear decorrelation and linear propagation times—is scale invariant, in the sense that the probability distribution of the ratio of these times is independent of scale. This result only holds if the local alignment of the Elsasser fields is taken into account in calculating the nonlinear time. At any given scale, the degree of alignment is found to increase with fluctuation amplitude, supporting the idea that the cause of alignment is mutual dynamical shearing of Elsasser fields. The scale-invariance of critical balance (while all other quantities of interest are strongly intermittent, i.e., have scale-dependent distributions) suggests that it is the most robust of the scaling principles used to describe Alfvénic turbulence. The quality afforded by situ fluctuation measurements in the solar wind allows for direct verification of this fundamental principle.

Key words: MHD—turbulence—solar wind

1 INTRODUCTION

Strong plasma turbulence is present in many astrophysical systems, and is directly measured by spacecraft in the solar wind (Bruno & Carbone 2005). The precision and sophistication achieved by these measurements in the recent years have enabled direct observational testing of theories of magnetized plasma turbulence that go beyond crude dimensional scalings—we mean, in particular, measurements of spatial anisotropy (Horbury et al. 2008; Podesta 2009; Wicks et al. 2010; Chen et al. 2011), intermittency (Horbury & Balogh 1997; Marsch & Tu 1997; Carbone et al. 2004; Salem et al. 2009; Zhdankin et al. 2012; Osman et al. 2014) and alignment (Podesta et al. 2009; Chen et al. 2012; Wicks et al. 2013a,b) of magnetic and velocity fluctuations. In this Letter, we report a new result, obtained numerically, that elicits a striking but physically plausible relationship between these three aspects of the structure of plasma turbulence.

In a strong mean magnetic field \mathbf{B}_0 , Alfvénic fluctuations decouple from compressive ones and satisfy the reduced magnetohydrodynamic (RMHD) equations, which correctly describe Alfvénic turbulence in both strongly and weakly collisional plasmas (see, e.g., Schekochihin et al. 2009, and references therein). The equations are best written in Elsasser (1950) variables $\mathbf{z}_\perp^\pm = \mathbf{u}_\perp \pm \mathbf{b}_\perp$, where \mathbf{u}_\perp and \mathbf{b}_\perp are the velocity and magnetic-field (in velocity units) perturbations, perpendicular to \mathbf{B}_0 :

$$\partial_t \mathbf{z}_\perp^\pm \mp v_A \partial_z \mathbf{z}_\perp^\pm + \mathbf{z}_\perp^\mp \cdot \nabla_\perp \mathbf{z}_\perp^\pm = -\nabla_\perp p, \quad (1)$$

where the pressure p is determined via $\nabla_\perp \cdot \mathbf{z}_\perp^\pm = 0$, $v_A = |\mathbf{B}_0|$ is the Alfvén speed, and \mathbf{B}_0 is in the z direction.

The modern understanding of the small-scale structure of Alfvénic turbulence described by equations (1) (and, indeed, the validity of these equations) rests on the fluctuations being spatially anisotropic with respect to the magnetic field, and ever more so at smaller scales—this is supported both by solar-wind measurements and by numerical simulations (see, e.g., Chen et al. 2011 and references therein). The relationship between the parallel and perpendicular coherence scales of the fluctuations is set via the *critical balance* conjecture (Goldreich & Sridhar 1995), whereby the nonlinear-interaction and the Alfvén-propagation times,

$$\tau_{\text{nl}}^\pm \doteq \frac{\lambda}{\delta z_\perp^\mp \sin \theta}, \quad \tau_A^\pm \doteq \frac{l_\parallel^\pm}{v_A}, \quad (2)$$

are expected to be comparable at each scale in some, shortly to be discussed, statistical sense. The Alfvén time is related solely to the scale l_\parallel^\pm of the the fluctuations along the magnetic field, while the nonlinear time depends on the fluctuation amplitudes δz_\perp^\pm , their scale λ perpendicular to the field and on the angle θ between $\delta \mathbf{z}_\perp^+$ and $\delta \mathbf{z}_\perp^-$ —when this angle is small, the nonlinearity in equations (1) is weakened, which is why we have included $\sin \theta$ in the definition of τ_{nl}^\pm . This effect that can become increasingly important at smaller scales as envisioned by the “dynamic alignment” conjecture (Boldyrev 2006; Mason et al. 2006) (its small-scale validity is, however, disputed in Beresnyak 2011, 2012).

Both the dynamics of weak turbulence ($\tau_A^\pm \ll \tau_{nl}^\pm$) and the causal impossibility to maintain $\tau_A^\pm \gg \tau_{nl}^\pm$ (fluctuations in planes perpendicular to \mathbf{B}_0 separated by a distance l decorrelate if l greatly exceeds the distance an Alfvén wave can travel during one nonlinear time, $l \gg v_A \tau_{nl}^\pm$) push the two time scales towards critical balance (Goldreich & Sridhar 1997; Boldyrev 2005; Nazarenko & Schekochihin 2011). This guarantees strong turbulence, with cascade time $\tau_c^\pm \sim \tau_{nl}^\pm \sim \tau_A^\pm$. Then, by the Kolmogorov argument, the scale independence of the energy fluxes,

$$\varepsilon^\pm \sim \frac{(\delta z_\perp^\pm)^2}{\tau_c} \sim \frac{(\delta z_\perp^\pm)^2 v_A}{l_\parallel^\pm} \sim \frac{(\delta z_\perp^\pm)^2 \delta z_\perp^\mp \sin \theta}{\lambda} \sim \text{const}, \quad (3)$$

immediately implies $\delta z_\perp^\pm \propto (l_\parallel^\pm)^{1/2}$, or, equivalently, the “parallel energy spectrum” $E(k_\parallel) \propto k_\parallel^{-2}$, indeed seen in both the solar wind and simulations (Horbury et al. 2008; Podesta 2009; Wicks et al. 2010; Chen et al. 2011; Beresnyak 2014a). The perpendicular scaling $\delta z_\perp^\pm \propto \lambda^\alpha$ is harder to establish as it depends on the scaling of $\sin \theta$ —there is a continued debate whether the numerical evidence supports dynamic alignment ($\alpha = 1/4$, Perez et al. 2012) or (at small enough scales) does not ($\alpha = 1/3$, Beresnyak 2014b).

As the resolution of such debates depends crucially on measuring precise scaling exponents, it is important to put the scaling formalism outlined above on a more precise footing. Indeed, what does “ \sim ” precisely mean in relations such as equation (3)? And how does one derive precise scaling laws on the basis of such relations?—precise in the sense of definite predictions about unambiguously defined statistical averages calculated from an ensemble (or a time history) of random solutions of equation (1).

That this is not a trivial question has long been known in the older field of hydrodynamic turbulence, where the statement $\varepsilon \sim \delta u^3/\lambda \sim \text{const}$, analogous to equation (3) (δu are velocity increments), does not imply $\langle \delta u^n \rangle \propto \lambda^{n/3}$ for any moment except $n = 3$ —a phenomenon of *intermittency* of turbulent fluctuations (Frisch 1995). Furthermore, ε is also an intermittent quantity: apart from $\langle \varepsilon \rangle$, no other moment of ε is scale-independent. Then “ $\varepsilon \sim \delta u^3/\lambda$ ” means that both sides have the same distribution, which depends on λ (“refined similarity hypothesis,” Kolmogorov 1962). We will adopt the same approach to equation (3), noting that, in Alfvénic turbulence, not only the amplitudes δz_\perp^\pm , but also l_\parallel^\pm and θ (all precisely defined below) are intermittent (have distributions that depend on λ *in a non-self-similar way*) and mutually *dependent* random variables.

In what follows, we will examine the joint statistical distribution of δz_\perp^\pm , l_\parallel^\pm and θ as a function of λ and show that critical balance is a more robust statistical statement than any other of the “ \sim ” relations—in the sense that the nonlinearity parameter

$$\chi^\pm \doteq \frac{\tau_A^\pm}{\tau_{nl}^\pm} = \frac{l_\parallel^\pm \delta z_\perp^\mp \sin \theta}{v_A \lambda}, \quad (4)$$

while still a random variable, has a distribution that is independent of scale. We call this statement, which in the “ \sim ” language could be written as $\chi^\pm \sim 1$, the *refined critical balance (RCB)*. We interpret it as evidence that critical balance results from a dynamical process that happens to inertial-

range fluctuations in a completely scale-invariant way. The presence of the alignment angle θ in equation (4) will turn out to be an essential feature of the RCB. We will also examine how the (non-scale-invariant) distributions of τ_A^\pm and τ_{nl}^\pm combine to give rise to a scale-invariant χ^\pm .

2 DEFINITIONS

We first define the quantities of interest. The fluctuation amplitudes are measured by increments

$$\delta z_\perp^\pm \doteq |\delta \mathbf{z}_\perp^\pm| \doteq |\mathbf{z}_\perp^\pm(\mathbf{r}_0 + \mathbf{r}_\perp) - \mathbf{z}_\perp^\pm(\mathbf{r}_0)|, \quad \lambda \doteq |\mathbf{r}_\perp|, \quad (5)$$

where \mathbf{r}_0 is an arbitrary point (irrelevant under averaging because turbulence is homogeneous) and \mathbf{r}_\perp the separation in the plane perpendicular to \mathbf{B}_0 (moments of δz_\perp^\pm only depend on λ because of global isotropy in the perpendicular plane). The alignment angle is given by

$$\sin \theta \doteq \frac{|\delta \mathbf{z}_\perp^+ \times \delta \mathbf{z}_\perp^-|}{\delta z_\perp^+ \delta z_\perp^-}. \quad (6)$$

The parallel coherence length l_\parallel^\pm corresponding to a perpendicular separation \mathbf{r}_\perp is defined as the shortest distance along the *perturbed* field line at which the Elsasser-field increment is the same as δz_\perp^\pm (Cho & Vishniac 2000; Maron & Goldreich 2001; Matthaeus et al. 2012):

$$\left| \mathbf{z}_\perp^\pm \left(\mathbf{r}_0 + \frac{\mathbf{r}_\perp + l_\parallel^\pm \hat{\mathbf{b}}_{\text{loc}}}{2} \right) - \mathbf{z}_\perp^\pm \left(\mathbf{r}_0 + \frac{\mathbf{r}_\perp - l_\parallel^\pm \hat{\mathbf{b}}_{\text{loc}}}{2} \right) \right| = |\mathbf{z}_\perp^\pm(\mathbf{r}_0 + \mathbf{r}_\perp) - \mathbf{z}_\perp^\pm(\mathbf{r}_0)|, \quad (7)$$

where $\hat{\mathbf{b}}_{\text{loc}} = \mathbf{B}_{\text{loc}}/|\mathbf{B}_{\text{loc}}|$ is the unit vector along the “local mean field” $\mathbf{B}_{\text{loc}} \doteq \mathbf{B}_0 + [\mathbf{b}_\perp(\mathbf{r}_0) + \mathbf{b}_\perp(\mathbf{r}_0 + \mathbf{r}_\perp)]/2$. Note that l_\parallel^\pm is a random quantity, *not* a parameter (unlike λ).

At each scale λ , the joint probability distribution function (PDF) $P(\delta z_\perp^+, \delta z_\perp^-, \theta, l_\parallel^+, l_\parallel^- | \lambda)$ contains all the information one customarily requires to characterize the structure of Alfvénic turbulence. As we only consider “balanced” turbulence, with equal mean injected power in the + and – fluctuations, P is symmetric with respect to the + and – variables. We will use the + mode wherever we need to make a choice. Imbalance leads to further interesting complications, left for future investigations.

3 NUMERICAL EXPERIMENT

We solved equations (1) using the code described in Chen et al. (2011) in a triply periodic box of resolution 1024^3 . In the code units, $v_A = 1$ and the box length = 2π in each direction. The RMHD equations are invariant with respect to simultaneous rescaling $z \rightarrow az$, $v_A \rightarrow av_A$ for arbitrary a . Therefore, although in code units the box is cubic and $\delta z_\perp^\pm/v_A \sim 1$, in fact the box is much longer in the parallel than in the perpendicular direction and the fluctuation amplitudes are much smaller than v_A , while the linear and nonlinear terms remain comparable. The energy was injected via white-noise forcing at $k_\perp = 1, 2$ and $k_\parallel = 1$ and dissipated by perpendicular hyperviscosity ($\nu_\perp \nabla_\perp^8$ with $\nu_\perp = 2 \times 10^{-17}$) and Laplacian viscosity in z ($\nu_z \partial^2/\partial z^2$ with $\nu_z = 1.5 \times 10^{-4}$; this is needed for numerical stability and has been checked to dissipate a negligible fraction of

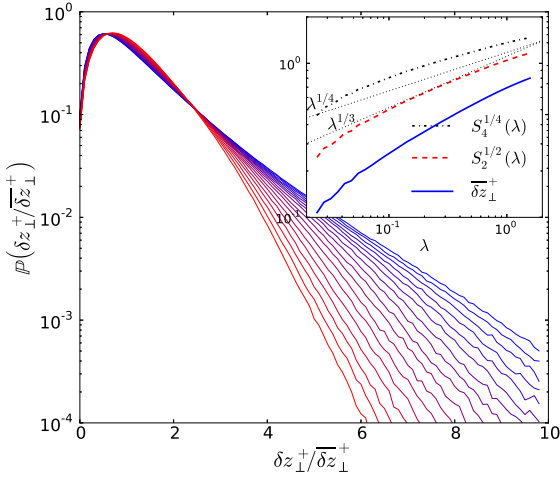


Figure 1. PDF of δz_{\perp}^{+} rescaled to $\overline{\delta z_{\perp}^{+}} \doteq \exp(\ln \delta z_{\perp}^{+} | \lambda)$, for scales from $\lambda = 0.094$ (blue/dark) to $\lambda = 0.92$ (red/light). *Inset:* the rms (2nd-order) increment $S_2^{1/2}(\lambda) \doteq \langle (\delta z_{\perp}^{+})^2 | \lambda \rangle^{1/2}$ (red dashed line), the 4th-order increment, $S_4^{1/4}(\lambda) \doteq \langle (\delta z_{\perp}^{+})^4 | \lambda \rangle^{1/4}$ (black dash-dotted line), and the “typical” increment $\overline{\delta z_{\perp}^{+}}$ (blue solid line); the slopes $\lambda^{1/4}$ (Boldyrev 2006) and $\lambda^{1/3}$ (Goldreich & Sridhar 1995) are given for reference; all increments are normalized to the overall rms fluctuation level.

energy). The mean injected power was $\epsilon^{\pm} = 1$ (balanced, strong turbulence). The forcing was purely in velocity; the magnetic field was not directly forced (we have checked that when the two Elsasser fields are forced independently, all results reported below continue to hold).

The field increments (5), angles (6) and parallel scales (7) were calculated for 32 logarithmically spaced scales, of which 17 were in the inertial range $0.094 \leq \lambda \leq 0.92$. For each λ , 10^6 point separations were generated by choosing a random initial point \mathbf{r}_0 on the grid and a random direction for \mathbf{r}_{\perp} uniformly distributed in angle over a circle of radius λ in the perpendicular plane. For each λ , the joint PDF P was averaged over 10 such samples of 10^6 , from snapshots separated by approximately one large-scale eddy turnover time.

4 RESULTS

4.1 Intermittency and Lack of Scale Invariance

A standard question of all turbulence studies is how the increments δz_{\perp}^{+} depend on λ . As we anticipated above, the answer depends on which moment of the distribution $P(\delta z_{\perp}^{+} | \lambda)$ we choose to calculate. As shown in figure 1 (inset) the rms increment $S_2^{1/2}(\lambda) \doteq \langle (\delta z_{\perp}^{+})^2 | \lambda \rangle^{1/2}$, based on the second-order structure function $S_2(\lambda)$, has a scaling between $\lambda^{1/3}$ (Goldreich & Sridhar 1995’s $k_{\perp}^{-5/3}$) and $\lambda^{1/4}$ (Boldyrev 2006’s $k_{\perp}^{-3/2}$), with the usual difficulty of distinguishing between two very close exponents in a finite-resolution simulation. In contrast, the geometric, rather than arithmetic, mean $\overline{\delta z_{\perp}^{+}} \doteq \exp(\ln \delta z_{\perp}^{+} | \lambda)$, perhaps better representing the “typical realization,” has a steeper scaling, whereas the “fourth-order increment” $S_4^{1/4}(\lambda) \doteq \langle (\delta z_{\perp}^{+})^4 | \lambda \rangle^{1/4}$ has a shallower one. The distribution is clearly not scale-invariant, as is

made manifest by figure 1, where we show $P(\delta z_{\perp}^{+} | \lambda)$ rescaled to $\overline{\delta z_{\perp}^{+}}$ at each λ . The salient feature of this PDF (which may be consistent with a lognormal, Zhdankin et al. 2012, or a log-Poisson, Chandran et al. 2014, distribution) is that it broadens at smaller λ —a classic case of intermittency understood as scale dependence of the distribution’s shape.

Other interesting quantities: θ , l_{\parallel}^{\pm} , τ_{A}^{\pm} , τ_{nl}^{\pm} , etc., also have intermittent, non-scale-invariant distributions. Let us focus on the two characteristic times.

4.2 Alfvén Time and Nonlinear Time

The distribution of $\tau_{\text{A}}^{\pm} = l_{\parallel}^{\pm} / v_{\text{A}}$ is simply the distribution of the parallel coherence length. Its geometric mean is shown in figure 2(a, inset) and appears consistent with the scaling $\overline{\tau_{\text{A}}^{+}} \doteq \exp(\ln \tau_{\text{A}}^{+} | \lambda) \propto \lambda^{1/2}$, which is the relationship between the parallel and perpendicular scales that would follow from Boldyrev’s phenomenology ($\delta z_{\perp}^{\pm} \propto \lambda^{1/4} \propto (l_{\parallel}^{\pm})^{1/2}$, Boldyrev 2006).¹ We see that it holds without being weighted by the fluctuation amplitude, i.e., it is a measure of the prevailing spatial anisotropy in the system. The PDFs of the rescaled quantity $\tau_{\text{A}}^{+} / \lambda^{1/2}$ for a range of λ are shown in figure 2(a): at smaller $\tau_{\text{A}}^{+} / \lambda^{1/2}$ (i.e., relatively shorter l_{\parallel}^{+}), there appears to be a scale-invariant collapse, but at larger values, the PDF becomes non-scale-invariant—with a systematically shallower tail at larger λ .

The geometric mean of the nonlinear time is shown in figure 2(b, inset) and, like $\overline{\tau_{\text{A}}^{+}}$, scales as $\overline{\tau_{\text{nl}}^{+}} \doteq \exp(\ln \tau_{\text{nl}}^{+} | \lambda) \propto \lambda^{1/2}$. Note that the presence of the alignment angle θ in the definition (2) of τ_{nl}^{\pm} is essential because it reduces the strength of the nonlinear interaction in a scale-dependent way. The PDFs of the rescaled inverse nonlinear time, $\lambda^{1/2} / \tau_{\text{nl}}^{+}$, are shown in figure 2(b). There is approximate (but clearly not perfect) scale invariance at small values of the rescaled quantity (i.e., relatively longer τ_{nl}), and a very non-scale-invariant tail at larger values, systematically shallower at smaller λ .

4.3 Refined Critical Balance

The behaviour of the distribution of the nonlinear time fits neatly with that of the distribution of the Alfvén time. The cores of both distributions (roughly, $\tau_{\text{A}}^{+} / \lambda^{1/2} \lesssim 3$ and $\lambda^{1/2} / \tau_{\text{nl}}^{+} \lesssim 3$ in figure 2) are close to being scale invariant. On the other hand, their tails vary with λ in opposite senses, with the tail of $\tau_{\text{A}}^{\pm} / \lambda^{1/2}$ ($\lambda^{1/2} / \tau_{\text{nl}}^{\pm}$) becoming steeper (shallower) as λ decreases. Because of this, the distribution of their product χ^{\pm} , defined in equation (4), does

¹ A more traditional way of extracting parallel scalings (corresponding to what is in fact done in the solar wind, Horbury et al. 2008; Podesta 2009; Wicks et al. 2010; Chen et al. 2011) is to define *parallel* increments $\delta z_{\perp}^{\pm} \doteq |\mathbf{z}_{\perp}^{\pm}(\mathbf{r}_0 + l_{\parallel} \hat{\mathbf{b}}_{\text{loc}}) - \mathbf{z}_{\perp}^{\pm}(\mathbf{r}_0)|$, where $\hat{\mathbf{b}}_{\text{loc}}$ is the local field direction at \mathbf{r}_0 and l_{\parallel} is a parameter, not a random variable. The rms of these increments is $\langle (\delta z_{\perp}^{\pm})^2 | l_{\parallel} \rangle^{1/2} \propto l_{\parallel}^{1/2}$ (Chen et al. 2011), which is reassuring as, replacing in equation (3) $\delta z_{\perp}^{\pm} \rightarrow \delta \tilde{z}_{\perp}^{\pm}$, $l_{\parallel}^{\pm} \rightarrow l_{\parallel}$ and averaging, we get $\langle (\delta \tilde{z}_{\perp}^{\pm})^2 \rangle \sim l_{\parallel} \langle \epsilon \rangle / v_{\text{A}}$, where the mean injected power $\langle \epsilon \rangle$ is certainly independent of scale.

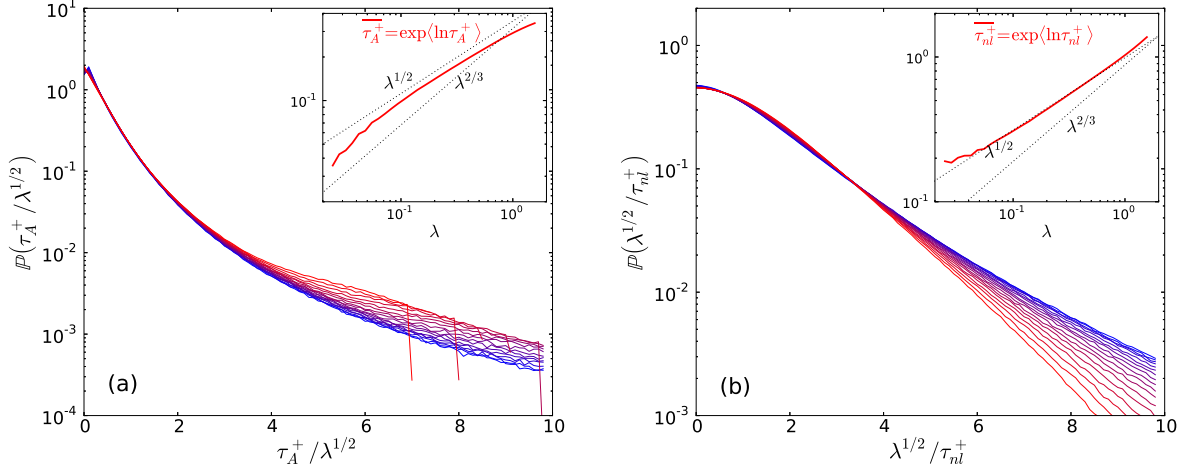


Figure 2. PDFs of (a) $\tau_A^+ \doteq l_{\parallel}^+ / v_A$ and (b) $(\tau_{nl}^+)^{-1}$ [equation (2)], rescaled by $\lambda^{1/2}$, for scales from $\lambda = 0.095$ (blue/dark) to $\lambda = 0.92$ (red/large). *Insets:* “Typical times” (a) $\bar{\tau}_A \doteq \exp(\ln \tau_A^+)$ and (b) $\bar{\tau}_{nl} \doteq \exp(\ln \tau_{nl}^+)$ vs. λ ; $\lambda^{1/2}$ and $\lambda^{2/3}$ scalings are shown for reference.

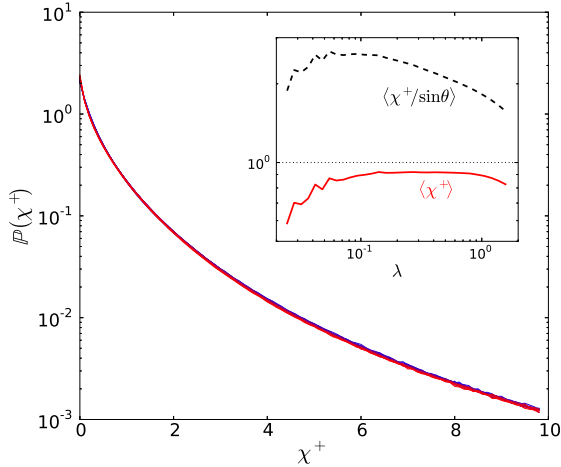


Figure 3. PDF of χ^+ (defined by equation (4)) for scales from $\lambda = 0.094$ (blue/dark) to $\lambda = 0.92$ (red/large). Data collapse is nearly perfect. *Inset:* the mean nonlinearity parameter $\langle \chi^+ \rangle$ vs. λ (red/solid) and the same without account for alignment, $\langle \chi^+ / \sin \theta \rangle$ (black/dashed).

not change at all: $P(\chi^+|\lambda)$, shown in figure 3, is independent of λ across the inertial range and all its moments are constant: e.g., $\langle \chi^+|\lambda \rangle$ is shown in the inset of figure 3 (alongside it, we show the mean nonlinearity parameter without the $\sin \theta$ factor, $\langle \chi^+ / \sin \theta | \lambda \rangle$; it is not scale-independent, so the alignment is an essential ingredient of the RCB).

That the nonlinearity parameter χ^{\pm} has a scale-invariant distribution is the main result of this Letter. This is due to the fundamental physical connection between the parallel and perpendicular structure of turbulent fluctuations—they cannot remain coherent beyond a parallel distance that information propagates at the Alfvén speed during one perpendicular nonlinear decorrelation time, $\tau_A^{\pm} \sim \tau_{nl}^{\pm}$.

4.4 Alignment

The role of alignment in giving rise to the RCB deserves further discussion. At every scale λ , the fluctuation amplitude δz_{\perp}^{\mp} and the alignment angle θ turn out to be *anticorrelated* (cf. Beresnyak & Lazarian 2006). This is best demonstrated by the conditional PDF $P(\sin \theta | \delta z_{\perp}^+ / \bar{\delta z}_{\perp}^+, \lambda)$, shown in figure 4. We see that fluctuations whose amplitudes are large relative to the “typical” value $\bar{\delta z}_{\perp}^+$ (i.e., those giving rise to the shallow intermittent tails manifest in figure 1) tend to be well aligned, whereas the weaker fluctuations ($\delta z_{\perp}^+ / \bar{\delta z}_{\perp}^+ \lesssim 1$) are unaligned. The alignment of the stronger fluctuations appears to get statistically “tighter” at smaller scales.

Thus, for the stronger fluctuations, the nonlinear interaction is reduced by alignment more than for the weaker ones. We find the approximately scale-invariant core of the distribution of $\lambda^{1/2} / \tau_{nl}^+$ in figure 2(b) to contain simultaneously smaller θ but relatively larger δz_{\perp}^- , so it is the more aligned fluctuations that give rise to the Boldyrev (2006) scaling $\delta z_{\perp}^+ \propto \lambda^{1/4}$, as expected. Note, however, that the anticorrelation between alignment and amplitude is somewhat at odds with Boldyrev’s intuitive interpretation of the alignment angle as determined by the maximal angular wander within any given fluctuation ($\theta \sim \delta b_{\perp} / B_0$), but rather suggests that alignment might be caused by dynamical shearing of a weaker Elsasser field by a stronger one (Chandran et al. 2014; the anticorrelation holds for both the weaker and the stronger of the two Elsasser fields, but is slightly more pronounced if figure 4 is re-plotted for $P(\sin \theta | \delta z_{\perp}^{(\max)} / \bar{\delta z}_{\perp}^{(\max)}, \lambda)$ with $\delta z_{\perp}^{(\max)}$ the locally stronger field). Qualitatively, this is why measures of alignment weighted by the energy (or higher powers of fluctuation amplitudes) exhibit stronger scale dependence (Beresnyak & Lazarian 2009; Mallet et al. 2014).

All of these statements must be accompanied by the acknowledgment that a debate continues as to whether the tendency to alignment in Alfvénic turbulence survives at asymptotically small scales, with numerical simulations at resolutions up to 4096^3 falling short of an indisputable out-

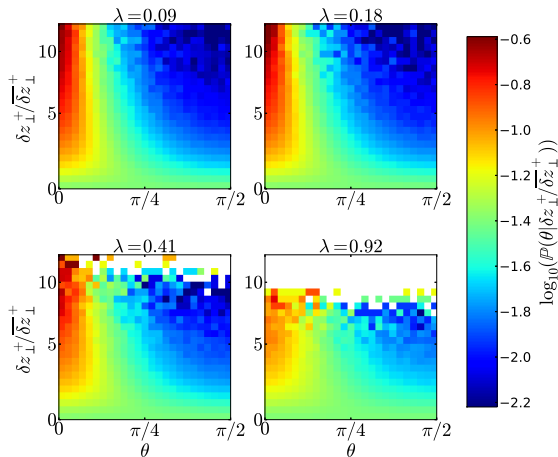


Figure 4. PDF of the alignment angle θ conditional on the fluctuation amplitude δz_{\perp}^{+} relative to “typical” value $\overline{\delta z_{\perp}^{+}} \doteq \exp\langle \ln \delta z_{\perp}^{+} | \lambda \rangle$, viz., $P(\sin \theta | \delta z_{\perp}^{+} / \overline{\delta z_{\perp}^{+}}, \lambda)$, plotted for four representative scales λ (as shown).

come (Perez et al. 2012; Beresnyak 2014b). What does, however, appear to be solidly the case is that Alfvénic fluctuations over at least the first two decades below the outer scale do exhibit alignment, even if transiently (cf. Podesta et al. 2009; Chen et al. 2012; Wicks et al. 2013a,b), that they do this in a systematic, scale- and amplitude-dependent fashion and, as argued above, that this effect must be taken into account in interpreting what it means, statistically, for these fluctuations to be in a critically balanced state. The possible change of regime at even smaller scales (Beresnyak 2014b) is left outside the scope of the present work.

5 CONCLUSION

The results presented above imply that the structure of Alfvénic turbulence is set by two fundamental effects: the critical balance, *which occurs in a scale-invariant fashion* (probably due to the upper limit on the parallel coherence length of turbulent fluctuations imposed by causality over a nonlinear decorrelation time), and systematic alignment of the higher-amplitude fluctuations (probably due to dynamical mutual shearing of Elsässer fields). The first of these results suggests that critical balance—quantitatively amounting, as we have argued, to the RCB conjecture—is the most robust and reliable of the physical principles undepinning theories of Alfvénic turbulence.

While scale-dependent alignment of inertial-range fluctuations in the solar wind is still in question (Podesta et al. 2009; Chen et al. 2012; Wicks et al. 2013a,b), measurements of the anisotropy/alignment/intermittency of these fluctuations directed at the verification of the RCB might help establish whether numerical and real plasma turbulence share the key structural properties and whether, therefore, debates and insights arising from the former have a useful contribution to make to the understanding of the latter.

We are grateful to A. Beresnyak, C. H. K. Chen, S. C. Cowley, T. S. Horbury, J. C. Perez, and R. T. Wicks

for many useful discussions of MH turbulence. AM was supported in part by STFC (UK), BDGC by NASA grants NNX11AJ37G and NNX12AB27G, NSF grant AGS-1258998. Simulations reported here used XSEDE, which is supported by the US NSF Grant ACI-1053575.

REFERENCES

- Beresnyak A., 2011, *Phys. Rev. Lett.*, 106, 075001
 Beresnyak A., 2012, *MNRAS*, 422, 3495
 Beresnyak A., 2014a, arXiv:1407.2613
 Beresnyak A., 2014b, *ApJ*, 784, L20
 Beresnyak A., Lazarian A., 2006, *ApJ*, 640, L175
 Beresnyak A., Lazarian A., 2009, *ApJ*, 702, 1190
 Boldyrev S., 2005, *ApJ*, 626, L37
 Boldyrev S., 2006, *Phys. Rev. Lett.*, 96, 115002
 Bruno R., Carbone V., 2005, *Living Rev. Solar Phys.*, 2, 4
 Carbone V., Bruno R., Sorriso-Valvo L., Lepreti F., 2004, *Planet. Space Sci.*, 52, 953
 Chandran B. D. G., Schekochihin A. A., Mallet A., 2014, arXiv:1403.6354
 Chen C. H. K., Mallet A., Schekochihin A. A., Horbury T. S., Wicks R. T., Bale S. D., 2012, *ApJ*, 758, 120
 Chen C. H. K., Mallet A., Yousef T. A., Schekochihin A. A., Horbury T. S., 2011, *MNRAS*, 415, 3219
 Cho J., Vishniac E. T., 2000, *ApJ*, 539, 273
 Elsasser W. M., 1950, *Phys. Rev.*, 79, 183
 Frisch U., 1995, *Turbulence*. Cambridge University Press, Cambridge
 Goldreich P., Sridhar S., 1995, *ApJ*, 438, 763
 Goldreich P., Sridhar S., 1997, *ApJ*, 485, 680
 Horbury T. S., Balogh A., 1997, *Nonlin. Proc. Geophys.*, 4, 185
 Horbury T. S., Forman M., Oughton S., 2008, *Phys. Rev. Lett.*, 101, 175005
 Kolmogorov A. N., 1962, *J. Fluid Mech.*, 13, 82
 Mallet A., et al., 2014, in preparation
 Maron J., Goldreich P., 2001, *ApJ*, 554, 1175
 Marsch E., Tu C.-Y., 1997, *Nonlin. Proc. Geophys.*, 4, 101
 Mason J., Cattaneo F., Boldyrev S., 2006, *Phys. Rev. Lett.*, 97, 255002
 Matthaeus W. H., Servidio S., Dmitruk P., Carbone V., Oughton S., Wan M., Osman K. T., 2012, *ApJ*, 750, 103
 Nazarenko S. V., Schekochihin A. A., 2011, *J. Fluid Mech.*, 677, 134
 Osman K. T., Kiyani K. H., Chapman S. C., Hnat B., 2014, *ApJ*, 783, L27
 Perez J. C., Mason J., Boldyrev S., Cattaneo F., 2012, *Phys. Rev. X*, 2, 041005
 Podesta J. J., 2009, *ApJ*, 698, 986
 Podesta J. J., Chandran B. D. G., Bhattacharjee A., Roberts D. A., Goldstein M. L., 2009, *J. Geophys. Res.*, 114, A01107
 Salem C., Mangeney A., Bale S. D., Veltri P., 2009, *ApJ*, 702, 537
 Schekochihin A. A., Cowley S. C., Dorland W., Hammett G. W., Howes G. G., Quataert E., Tatsuno T., 2009, *ApJS*, 182, 310
 Wicks R. T., Horbury T. S., Chen C. H. K., Schekochihin A. A., 2010, *MNRAS*, 407, L31

Wicks R. T., Mallet A., Horbury T. S., Chen C. H. K.,
Schekochihin A. A., Mitchell J. J., 2013a, *Phys. Rev.*
Lett., 110, 025003

Wicks R. T., Roberts D. A., Mallet A., Schekochihin A. A.,
Horbury T. S., Chen C. H. K., 2013b, *ApJ*, 778, 177

Zhdankin V., Boldyrev S., Mason J., 2012, *ApJ*, 760, L22